

PAPER • OPEN ACCESS

## Cluster-shell model: I. Structure of ${}^9\text{Be}$ , ${}^9\text{B}$

To cite this article: Valeria Della Rocca and Francesco Iachello 2018 *J. Phys.: Conf. Ser.* **966** 012039

View the [article online](#) for updates and enhancements.

### Related content

- [Measurement of  \${}^2\text{H}\({}^6\text{Li}, {}^9\text{Be}\)\$  Reaction Relevant to Primordial Nucleosynthesis](#)  
Zeng Sheng, Liu Wei-Ping, Li Zhi-Hong et al.
- [Cluster-shell competition in light nuclei—inclusion of non-central interactions in -cluster model](#)  
N Itagaki
- [Quasielastic Scattering of the Halo Nucleus  \${}^6\text{He}\$  at 25 MeV/u from a  \${}^9\text{Be}\$  Target](#)  
Pang Dan-Yang, Ye Yan-Lin, Jiang Dong-Xing et al.

# Cluster-shell model: I. Structure of ${}^9\text{Be}$ , ${}^9\text{B}$

Valeria Della Rocca<sup>1,2</sup> and Francesco Iachello<sup>2</sup>

<sup>1</sup>Gran Sasso Science Institute, viale Francesco Crispi 7, 67100 L'Aquila, Italy

<sup>2</sup>Center for Theoretical Physics, Sloane Laboratory, Yale University, New Haven, CT 06520-8120, USA

E-mail: [valeria.dellarocca@gssi.it](mailto:valeria.dellarocca@gssi.it), [valeria.dellarocca@yale.edu](mailto:valeria.dellarocca@yale.edu),  
[francesco.iachello@yale.edu](mailto:francesco.iachello@yale.edu)

**Abstract.** A cluster-shell model suitable for the description of light nuclei seen as  $k$   $\alpha$ -particles +  $x$  nucleons is described. Its application to  ${}^9\text{Be}$  and  ${}^9\text{B}$  is also shown, for which we explicitly provide a comparison with the available experimental data.

## 1. Introduction

The cluster description of light nuclei was originally proposed in 1937 by Wheeler [1] and independently by Hafstad and Teller [2] in 1938, as a consequence of the observation of the high binding energy of the  ${}^4\text{He}$  nucleus. Specific cluster configurations were suggested by Brink [3, 4]. Following recent experimental developments [5], this model has regained interest. Indeed, it was found that the spectra of  ${}^8\text{Be}$ ,  ${}^{12}\text{C}$  and  ${}^{16}\text{O}$  are well reproduced by 2, 3 and 4 cluster configurations with  $Z_2$ ,  $D_{3h}$  and  $T_d$  symmetry respectively. An extension of this idea consists in the inclusion of an extra particle moving in the potential generated by the clusters. In this contribution, we will first describe the recently introduced cluster-shell model (CSM) [6], which we propose as a possible model to describe light even-odd nuclei with a cluster core, and then show its explicit application in the case of  ${}^9\text{Be}$  and  ${}^9\text{B}$ .

## 2. Cluster shell model

In previous works, the charge and matter density  $\rho(\vec{r})$  of 2, 3, and 4  $\alpha$ -particles have been found [6]. The convolution:

$$V(\vec{r}) = \int \rho(\vec{r}')v(\vec{r} - \vec{r}')d^3\vec{r}'. \quad (1)$$

of  $\rho(\vec{r})$  and the interaction between the  $\alpha$  and the nucleon,  $v(\vec{r} - \vec{r}')$ , which we assume to be of Volkov-type [7], allows the determination of the potential  $V(\vec{r})$  in which the odd nucleon is moving. Explicit calculation leads to [6]

$$V(\vec{r}) = V_0 e^{-\alpha(r^2 + \beta^2)} 4\pi \sum_{\lambda\mu} i_\lambda(2\alpha\beta r) Y_\mu^\lambda(\theta, \phi) \sum_i^k Y_\mu^{*\lambda}(\theta_i, \phi_i) \quad (2)$$

where  $i_\lambda$  is the modified spherical Bessel function. The  $\alpha$ -particles are assumed to be placed at positions  $r_i = (\beta, \theta_i, \phi_i)$  which are chosen according to the desired symmetry we wish to reproduce.



The single particle energies  $\epsilon_\Omega$  of a particle in the cluster potential in equation (2) are obtained by solving the Schrödinger equation:

$$H = \frac{\vec{p}^2}{2m} + V(\vec{r}) + V_{so}(\vec{r}) \quad (3)$$

where  $V_{so}(\vec{r})$  is the spin-orbit interaction, which we assume of the form:

$$V_{so}(\vec{r}) = V_{0,so} \frac{1}{r} \frac{\partial V}{\partial r} (\vec{s} \cdot \vec{l}) \quad (4)$$

Hence, the problem is essentially that of a particle in potentials that change in a continuous manner from having spherical symmetry to having point group symmetries,  $Z_2$  ( $k = 2$ ),  $D_{3h}$  ( $k = 3$ ),  $T_d$  ( $k = 4$ ), as the distance of the clusters  $\beta$  increases. Since the dimension of these discrete groups is smaller than the dimension of the rotation group, we expect each level to split according to the splitting of the representation of  $O(3)$  in terms of the irreducible representations of the point groups of interest.

We have diagonalized the Hamiltonian  $H$  in equation (3) numerically in the harmonic oscillator basis. The correlation diagrams corresponding to  $k = 2$ ,  $k = 3$ , and  $k = 4$  are depicted in figures 1, 2 and 3, respectively [6]. The states are labelled with the notation of the spherical shell model in  $\beta = 0$ . For  $\beta > 0$ , in the case of  $k = 2$  we have labelled the states with the projection of the angular momentum along the symmetry axis,  $K$ , and the parity,  $P$ , as well as with the molecular physics notation, while for  $k = 3, 4$  we have used the labels of the irreducible representations of  $D_{3h}$  and  $T_d$ , respectively. In figures 1 to 3 we also show that bigger gaps occur at different energies for different values of  $\beta$ .

### 3. Application to ${}^9\text{Be}$

The treatment of  ${}^9\text{Be}$  is a straightforward application of the model described so far, where the core is assumed to have the particular configuration depicted in figure 4, i.e. when  $k = 2$  and  $\beta = 1.82$  fm. The value of  $\beta$  has been derived from the experimental moment of inertia of  ${}^8\text{Be}$ . This particular configuration can be obtained choosing in equation (2)  $\vec{r}_1 = (r_1, \theta_1, \phi_1) = (\beta, 0, -)$  and  $\vec{r}_2 = (r_2, \theta_2, \phi_2) = (\beta, \pi, -)$  as the locations of the two  $\alpha$ -particles.

The single particle states and wave functions are obtained as explained in Sect. 2. Using the standard expression for rotational bands for axially symmetric nuclei [8]

$$E(J) = \epsilon_K + \frac{(\hbar c)^2}{2\mathcal{I}} \left[ J(J+1) - K^2 + \delta_{(K,1/2)} a(-)^{J+1/2} \left( J + \frac{1}{2} \right) \right] \quad (5)$$

we obtain the energy levels in figure (5), where the moment of inertia  $\mathcal{I}$  is the sum of the core and single particle contributions.

The electric transition rates,  $B(E\lambda)$ , and multipole electric moments,  $Q^{(\lambda)}(K, I)$ , with  $\lambda = 2, 4, \dots = \text{even}$  are dominated by the core contribution, while those with  $\lambda = 1, 3, \dots = \text{odd}$  between states with different parity (i.e. from the  $K^P = 1/2^+$  band excited states to  $K^P = 3/2^-$  ground state) are the sum of collective and single particle contributions. In the latter case, expanding the wave function in the h.o. basis:

$$|\psi\rangle = \sum_{nljm} a_{nljm} |n, \frac{1}{2}, l, j, m\rangle \quad (6)$$

we can evaluate the matrix elements of the operators defining the single particle contribution to moments and electric transition rates. The result has to be summed to the core contribution,

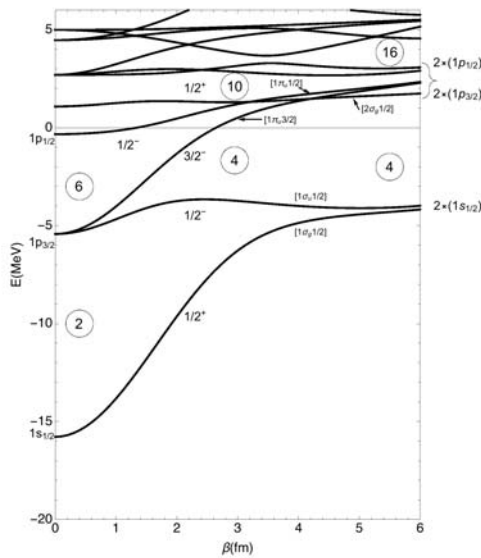


**Figure 1.** Correlation diagrams of the energy levels of a spin 1/2 particle for the potential in equation (2) as function of the distance  $\beta$  between the clusters and the center of mass for:  $k = 2$ . The parameters used are:  $V_0 = 20$  MeV,  $V_{0,so} = 22$  MeVfm<sup>2</sup>,  $\alpha = 0.1115$  fm<sup>-2</sup>. Reproduced from Ref. [6] with permission.

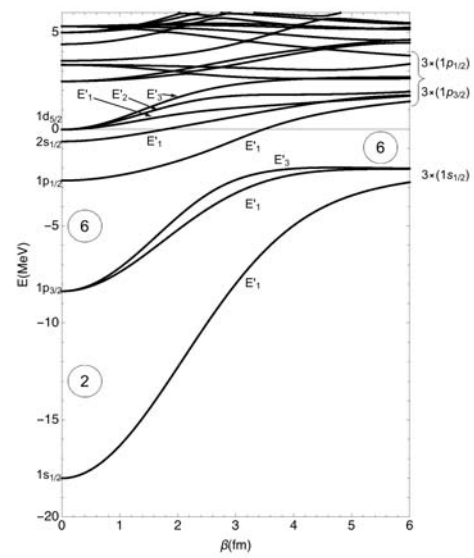


**Figure 2.** Correlation diagrams of the energy levels of a spin 1/2 particle for the potential in equation (2) as function of the distance  $\beta$  between the clusters and the center of mass for  $k = 3$ . The parameters used are:  $V_0 = 13.3$  MeV,  $V_{0,so} = 16.9$  MeVfm<sup>2</sup>,  $\alpha = 0.0872$  fm<sup>-2</sup>. Reproduced from Ref. [6] with permission.

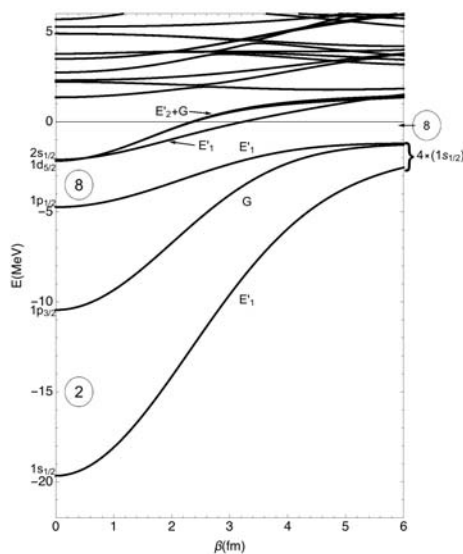


**Figure 3.** Correlation diagrams of the energy levels of a spin 1/2 particle for the potential in equation (2) as function of the distance  $\beta$  between the clusters and the center of mass for  $k = 4$ . The parameters used are:  $V_0 = 10$  MeV,  $V_{0,so} = 13.4$  MeVfm<sup>2</sup>,  $\alpha = 0.0729$  fm<sup>-2</sup>. Reproduced from Ref. [6] with permission.

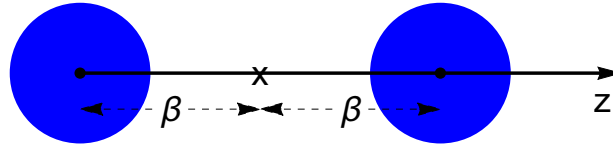


**Figure 4.**  $^8\text{Be}$  seen as two  $\alpha$ -particles in a dumbbell configuration.

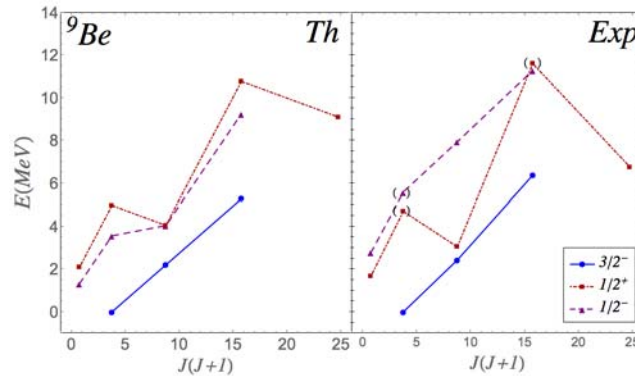


**Figure 5.** Comparison between (a) theory and (b) experiment of the energy levels of  $^9\text{Be}$ . Adapted from Ref. [11].

**Table 1.** Comparison between ( $e, e'$ ) [10], NDT [9], shell model (SM) and cluster shell model (CSM) calculations. Units of  $Q$  are in  $\text{efm}^2$  and of  $B(E2)$  are in  $\text{e}^2\text{fm}^4$ .

	( $e, e'$ )	NDT	SM	CSM
$Q^{(2)}(3/2^-)$	5.86(6)	5.288(38)	4.35	5.30
$B(E2; 3/2^- \rightarrow 5/2^-)$	46.0(5)	40.5(30)	32.2	35.9
$B(E2; 3/2^- \rightarrow 7/2^-)$	33(1)	18(8)	12.7	20.0

which is obtained by coupling single particle and core transition operators. Similar considerations hold for magnetic transition rates,  $B(M\lambda)$ , and magnetic moments,  $\mu^{(\lambda)}(K, I)$ . The explicit derivation of these quantities is rather long and therefore not reported here, but it can be found in [11, 12].

In table 1 we show the comparison between theory and experiment [9, 10] for the quadrupole moment of the ground state and for  $B(E2)$  transitions. The large value of  $Q^{(2)}(3/2^-)$  that we have obtained in the CSM is in good agreement with the existing data, a feature that is difficult to explain in a spherical model. Similarly, the large  $B(E2)$  values are a proof of collective structure of the system, being these transitions mostly due to the contribution of the core. This is a quite remarkable result, since we did not introduce any effective charge in the calculation.

Although smaller than the data from electron scattering, Ref. [10], the  $B(E1)$  transition rates, table 2, are in agreement with the Nuclear Data Tables (NDT) [9].

The magnetic moment of the ground state,  $\mu(3/2^-)$ , is also in fairly good agreement with the experiments, while  $B(M1; 3/2^- \rightarrow 5/2^-)$  is smaller, although of the same order of magnitude (see table 3 for comparison).

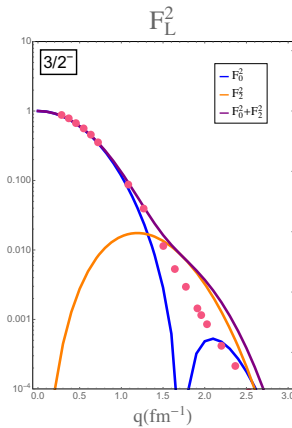
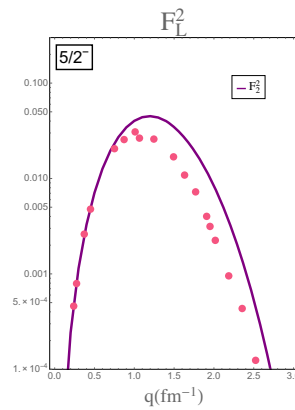
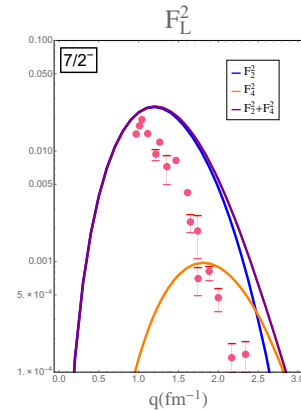
In figures 6 to 8 we show the longitudinal electric form factors relative to members of the

**Table 2.** Comparison between  $(e, e')$  [10], NDT [9], shell model (SM) and cluster shell model (CSM) calculations. Units are in  $e^2\text{fm}^2$ .

	$(e, e')$	NDT	SM	CSM
$B(E1; 3/2^- \rightarrow 1/2^+)$	0.034(3)	0.029(3)	0.0045	0.024
$B(E1; 3/2^- \rightarrow 5/2^+)$	0.029(5)	0.015(12)	0.0039	0.0048

**Table 3.** Comparison between  $(e, e')$  [10], NDT [9], shell model (SM) and cluster shell model (CSM) calculations. Units of magnetic moment are in  $\mu_N$  and of  $B(M1)$  those of Ref. [10],  $e^2\text{fm}^2$ .

	Exp( $e, e'$ )	NDT	SM	CSM
$\mu(3/2^-)$	-1.16(2)	-1.1778(9)	-1.27	-1.13
$B(M1; 3/2^- \rightarrow 5/2^-)$	0.0090(3)	0.0089(9)	0.0068	0.0038

**Figure 6.** Longitudinal electric form factor of the state  $3/2^-$ . Adapted from Ref. [12].**Figure 7.** Longitudinal electric form factor of the state  $5/2^-$ . Adapted from Ref. [12].**Figure 8.** Longitudinal electric form factor of the state  $7/2^-$ . Adapted from Ref. [12].

ground state band. For small values of the momentum transfer  $q$  the CSM reproduces the experimental results well, while as  $q$  increases it does not. This is expected, since for high momentum transfer one probes the inner structure of the  $\alpha$ -particle.

Our conclusion is that the cluster structure of  $^8\text{Be}$  is not destroyed when an extra fermion is added, i.e.  $^9\text{Be}$  can be seen as made of a core of  $2\alpha$ -particles plus an additional neutron.

#### 4. Application to $^9\text{B}$

The treatment of  $^9\text{B}$  in CSM is identical to that of  $^9\text{Be}$ , except that equation (3) is replaced by:

$$H = \frac{\vec{p}^2}{2m} + V(\vec{r}) + V_{so}(\vec{r}) + V_C(\vec{r}) \quad (7)$$

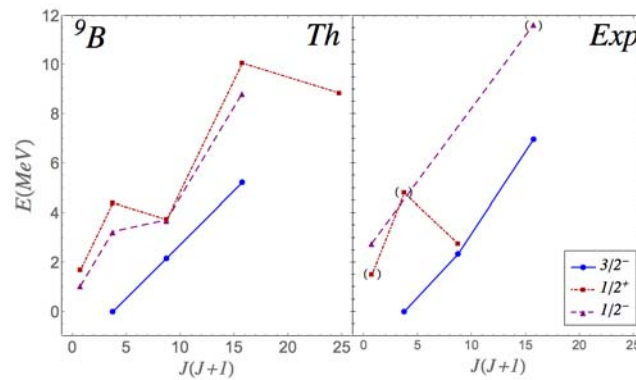


**Figure 9.** Rotational spectra of  ${}^9\text{B}$ . Adapted from Ref. [11].

where  $V_C(\vec{r})$  is the Coulomb potential generated by the density distribution of [6]. Figure 9 shows a comparison between the energy levels calculated using the CSM and the experimental data [9]. However, being  ${}^9\text{B}$  unstable, a comparison between CSM and experiment for  $B(E\lambda)$  and  $B(M\lambda)$  rates is not possible at present, due to the lack of experimental data. We have nonetheless evaluated such quantities for future reference and reported them in [12].

### Acknowledgments

This work was supported in part by US Department of Energy Grant No. DE-FG-02-91ER-40608, and, in part, by the Gran Sasso Science Institute (GSSI).

### References

- [1] Wheeler J A 1937 *Phys. Rev.* **52** 1083
- [2] Hafstad L R and Teller E 1938 *Phys. Rev.* **54** 681
- [3] Brink D M 1965 *Proc. Int. School of Physics "Enrico Fermi" Course XXXVI* p 247
- [4] Brink D M, Friedrich H, Weiguny A, and Wong C W 1970 *Phys. Lett. B* **33** 143
- [5] Marín-Lámbarri D J, Bijker R, Freer M, Gai M, Kokalova Tz, Parker D J, and Wheldon C 2014 *Phys. Rev. Lett.* **113** 012502
- [6] Della Rocca V, Bijker R and Iachello F 2017 *Nucl. Phys. A* **966** 158
- [7] Volkov A B 1965 *Nucl. Phys.* **74** 33
- [8] Rowe D J 2010 *Nuclear Collective Motion* (Singapore: World Scientific)
- [9] Tilley D R et al. 2004 *Nucl. Phys. A* **745** 155
- [10] Glickman J P et al. 1991 *Phys Rev. C* **43** 1740
- [11] Della Rocca V and Iachello F submitted to *Nucl. Phys. A*
- [12] Della Rocca V 2017 *Ph.D. thesis* Gran Sasso Science Institute (L'Aquila, Italy: GSSI)